Doctoral Dissertation
博士論文

Functional analysis of the *DWARF WITH SLENDER LEAF1* gene that plays diverse roles in development of *Oryza sativa*

（イネの発生に多面的に作用する *DWARF WITH SLENDER LEAF1* 遺伝子の機能解析）

A Dissertation Submitted for the Degree of Doctor of Philosophy
August 2019
令和元年８月博士（理学）申請

Department of Biological Sciences, School of Science,
The University of Tokyo
東京大学大学院理学系研究科生物科学専攻

Fumika Kubo
久保 文香

Contents

Acknowledgements

First of all, I would like to express my sincerest appreciation to Dr. Hiro-Yuki Hirano for his in-depth discussion and thoughtful encouragement on this study. I would also like to thank Dr. Ichiro Terashima, Dr. Kyoko Ohashi-Ito, Dr. Tetsuji Kakutani and Dr. Jun-Ichi Itoh (Graduate School of Agricultural and Life Sciences, The University of Tokyo) for their incisive comments and constructive suggestions on my thesis.

I am also very grateful to all the past and present members of the Laboratory of Evolutionary Genetics. I especially thank Dr. Yukiko Yasui for her useful advice and warm support; Dr. Wakana Tanaka for her technical guidance and kind support; Ms. Akiko Takahashi for her technical assistance.

I would like to thank my cooperators: Dr. Toshihiro Kumamaru (Kyushu University) for providing plant materials; Dr. Masaki Endo and Mr. Masafumi Mikami (National Institute of Agrobiological Sciences) for providing the pU6gRNA-oligo and pZH_OsU3gYSA_MMCas9 vectors; Dr. Kyoko Ohashi-Ito and Ms. Yukiko Sugisawa for microarray analysis; Dr. Yoshihiro Ohmori (Graduate School of Agricultural and Life Sciences, The University of Tokyo) for microarray data analysis; Dr. Ken-Ichi Nonomura, Mr. Mitsugu Eiguchi (National Institute of Genetics), and technicians at the Institute for Sustainable Agro-ecosystem Services of the University of Tokyo for cultivating rice.

Lastly, I thank my family for their continuous support and encouragement.

This study was supported in part by a Research Fellowship for Young Scientists from the Japan Society for the Promotion of Science.

List of Abbreviations

AS1	ASYMMETRIC LEAVES1
ASP1	ABERRANT SPIKELET AND PANICLE1
CDKB2	cyclin-dependent kinase B2
COW1	CONSTITUTIVELY WILTED1
CRISPR/Cas9	clustered regularly interspaced short palindromic repeats/ CRISPR-associated protein 9
DSL1	DWARF WITH SLENDER LEAF1
gRNA	guide RNA
HAT	histone acetyl transferase
HDAC	histone deacetylase
LG model	Le and Gascuel model
LSY1	LEAF LATERAL SYMMETRY1
LV	large vascular bundle (or vein)
ML	Maximum Likelihood
NAL	NARROW LEAF
ND1	NARROW LEAF AND DWARF1
NNI	nearest- neighbor-interchange

OLI1/HOS15	OLIGOCELLULA1/HIGH EXPRESSION OF OSMOTICALLY RESPONSIVE GENES15
PN	penultimate leaf
PWR	POWERDRESS
RPD3/HDA1 family	Reduced potassium dependence3/Histone Deacetylase1 family
SAM	shoot apical meristem
SIR2 family	Silent Information Regulator 2
SLE1	SLENDER LEAF1
SV	small vascular bundle (or vein)
TAW1	TAWAWA1
TPL	TOPLESS
WT	wild type

Abstract

Plant development is governed by the activity of the meristem. Lateral organs such as the leaf and flower are developed by cells supplied from stem cells at the peripheral region of the meristem. A lot of genes that regulate the meristem activity and the organ differentiation in plant development have been reported so far. However, the molecular mechanisms underlying the generation of the morphological diversities of angiosperms are not fully understood. Rice (*Oryza sativa*), a model plant of the monocots, had unique morphological characteristics. Rice leaves consist of the leaf blade and leaf sheath, which are connected by a boundary region (lamina joint), and have parallel longitudinal veins. In the reproductive phase, the inflorescence meristems generate branches, and then the branch meristems produce spikelets. A variety of genes that regulate flower and inflorescence development have been identified, and the primary molecular mechanism such as that shown by the ABC model is conserved in rice. However, further researches are necessary to understand the developmental mechanism underlying the construction of morphology specific to rice plant. Thus, I aimed to elucidate a new gene that is involved in rice development and to gain some insights for understanding the function of genes related to distinct morphologies of rice. In this thesis, I focus on a

novel rice mutant, *dwarf with slender leaf1* (*dsl1*), which exhibited pleiotropic defects in both vegetative and reproductive development.

In the vegetative phase, the lengths of both the leaf blade and leaf sheath were shorter in the *dsl1* mutant as compared to wild type. I also found that the width of the leaf blade was narrower in *dsl1* than in wild type. In association with the narrow width, both the number of the longitudinal veins and the distance between them were reduced in *dsl1*. My histological analysis suggested that a reduction in cell number rather than cell size seems to be a cause of the shorter distance between the longitudinal veins in *dsl1*. In addition, the reduced size of the vascular bundle also resulted from a decrease in the number of cells.

I hypothesized that the morphological defects of the leaf of the *dsl1* mutant are related to the abnormality of cell division. Then, I analyzed the spatial expression pattern of *cyclin-dependent kinase B2* (*CDKB2*), a marker of the cell cycle. As a result, the level of *CDKB2* expression was reduced in the leaf primordia in *dsl1*. In addition, the number of cells expressing *CDKB2* was also decreased. These results suggested that the regulation of the cell cycle was partially disturbed in the leaf primordia of *dsl1*. I also found that the shoot apical meristem (SAM) shape in *dsl1* was slightly different from that in wild type. In consequence, the early stage

of leaf development and the SAM maintenance seems to be affected in *dsl1*.

Next, I observed the phenotypes of the *dsl1* mutant in the reproductive phase. I first revealed that apparent semi-dwarfism in *dsl1* resulted from the shortening of the upper internodes, as compared with wild type. In addition, the internode patterning was unique in *dsl1*, because the elongation of the lower internodes was slightly promoted. I also found that the panicles and spikelets of *dsl1* were smaller than those of wild type. Moreover, some of the terminal spikelets replaced by abnormal appendages. These results suggest that the activities of both the inflorescence and branch meristems are reduced in *dsl1*. Furthermore, the *dsl1* spikelet showed low fertility and impaired anthers.

Gene isolation by the combination of positional cloning and next-generation sequencing revealed that *DSL1* encodes a histone deacetylase (HDAC) (Os04g0409600) belonging to the Class I of the Reduced potassium dependence3 /Histone Deacetylase1 (RPD3/HDA1) family. To confirm that *DSL1* is Os04g0409600, I made and observed the knockout mutant of Os04g0409600 by using CRISPR-Cas9 technology. This knockout mutant represented the various morphological abnormalities similar to those observed in *dsl1*. Therefore, I concluded that *DSL1* is Os04g0409600.

To know the function of *DSL1*, I examined the organ-specific expression of *DSL1* by RT-PCR. Consistent with the pleiotropic alterations observed in *dsl1*, the expression of *DSL1* detected in a variety of organs and developmental stages.

In this thesis, I revealed that *DSL1* encodes an HDAC and plays various roles in rice development. To my knowledge, how HDACs contribute to the development of rice is poorly understood, and the *dsl1* mutant is the first mutant that reported as the loss-of-function of an HDAC of the RPD3/HDA1 family. In the future, it will be interesting to elucidate how DSL1 regulates such various developmental processes in rice and to identify the other proteins acting together with DSL1 and those controlled by DSL1.

Chapter I

Introduction

Plant development is governed by the activity of the shoot apical meristem (SAM), where stem cells are maintained (Ha et al. 2010; Aichinger et al. 2012; Somssich et al. 2016). Lateral organs such as the leaf and flower differentiate from cells supplied from stem cells at the peripheral region of the meristem. During organ development, three developmental axes (apical–basal, adaxial–abaxial, and centrolateral axis) are established and specific types of cell differentiate along these axes.

Plant architecture depends on the shape and size of the lateral organs and the arrangement of the secondary shoots. Rice (*Oryza sativa*) reiteratively generates leaves and secondary shoots in the vegetative phase (Hoshikawa 1989; Itoh et al. 2005). Because the stem does not elongate in either the primary or secondary shoots during this phase, the apparent architecture of rice is influenced by the shape and size of the leaves. After flower induction, the vegetative SAM changes its properties and becomes the inflorescence meristem, which generates inflorescences consisting of branches and spikelets (Tanaka et al. 2013). The shape and size of these inflorescences affect plant architecture in the reproductive phase.

Rice leaves consist of the leaf blade and leaf sheath, which are connected by a

boundary region (lamina joint) harboring the ligule and auricle (Hoshikawa 1989). In the leaf blade, two types of longitudinal vascular bundle, termed large and small, differentiate to transport water and nutrients. Relative to the small vascular bundle, the large bundle contains many cells and different types of cells. Viewed from the outside, the two types of vascular bundle are visible as large and small veins, with 5–6 small veins between the large veins in wild type.

Leaf morphogenesis and regulation of leaf size have been studied by using narrow leaf mutants such as *narrow leaf2* (*nal2*), *nal3*, *nal7/constitutively wilted1* (*cow1*), *leaf lateral symmetry1* (*lsy1*), and *slender leaf1* (*sle1*)*/narrow leaf and dwarf1* (*nd1*) (Woo et al. 2007; Fujino et al. 2008; Li et al. 2009; Cho et al. 2013; Ishiwata et al. 2013; Yoshikawa et al. 2013; Kubo et al. 2017; Honda et al. 2018). The narrow width of the leaf blade is associated with a decrease in the number of either large or small veins. The pattern of reduction observed for each vein varies depending on the narrow leaf mutants, suggesting that the formation pattern of the large and small veins is regulated genetically. The genes responsible for these mutations encode proteins associated with transcriptional regulation, auxin biosynthesis, and cellulose synthesis (Woo et al. 2007; Fujino et al. 2008; Li et al. 2009; Cho et al. 2013; Ishiwata et al. 2013; Yoshikawa et al. 2013; Kubo et al. 2017; Honda et al. 2018). Thus, many genes

regulating various biological activities are involved in leaf morphogenesis and regulation of leaf size.

In the reproductive phase, the inflorescence meristem generates primary branch meristems instead of leaf primordia in the peripheral region (Tanaka et al. 2013). The inflorescence meristem also supplies cells just below the meristem to form the inflorescence stem (culm) (Hoshikawa 1989; Sato et al. 1999). The culm is composed of several internodes. The nodes and internodes differentiate at an early stage of inflorescence development, and the internodes elongate gradually, resulting in the heading of the inflorescence (panicle). The elongation of each internode is regulated independently because dwarf mutants display distinct patterns of internode elongation as classified by Takeda (1977). Recent studies have shown that internode elongation is regulated by various types of gene, encoding, for example, transcription factors specifying cell type and enzymes catalyzing gibberellin and brassinosteroid biosynthesis (Sato et al. 1999; Yamamuro et al. 2000; Sasaki et al. 2002). Semi-dwarf phenotype is an important agronomic trait, because semi-dwarf varieties are associated with a high yield in rice, as well as wheat (Sasaki et al. 2002).

The branch meristem generated by the inflorescence meristem then produces both spikelets and secondary branch meristems at the peripheral region (Tanaka et al.

2013). The branch meristem ultimately converts into the spikelet meristem, which forms the terminal spikelet. Thus, terminal spikelets are formed by a different developmental process as compared with the lateral spikelets, which differentiate from the meristem formed at the periphery of the branch meristem. The timing of the transition from the indeterminate branch meristem to the determinate spikelet meristem is related to inflorescence size. *TAWAWA1* (*TAW1*) negatively regulates meristem fate, and a gain-of-function mutant of *TAW1* generates highly-branched large inflorescences (Yoshida et al. 2013). By contrast, small inflorescences with short primary branches are formed in the *aberrant spikelet and panicle1* (*asp1*) mutant, which has partial defects in meristem maintenance (Yoshida et al. 2012).

Reversible histone acetylation and deacetylation are important epigenetic codes in eukaryotic gene regulation. In general, histone acetylation is associated with gene activation because it opens up the chromatin structure, whereas histone deacetylation is associated with gene silencing because it closes the chromatin. Histone deacetylation is catalyzed by histone deacetylases (HDACs) (Kadosh and Struhl 1998; Rundlett et al. 1998), which are grouped into three families: Reduced potassium dependence3/Histone Deacetylase1 (RPD3/HDA1), Histone Deacetylase 2 (HD2), and Silent Information Regulator 2 (SIR2) (Pandey et al. 2002; Hollender and Liu

2008). The RPD3/HDA1 and SIR2 families are widely conserved in eukaryotes, whereas the HD2 family is plant-specific. The RPD3/HDA1 family is further divided into several classes, such as class I and class II (Pandey et al. 2002; Fu et al. 2007; Hollender and Liu 2008; Alinsug et al. 2009; Liu et al. 2014; Liu et al. 2016).

Histone deacetylases in the RPD3/HDA1 family play roles in a wide range of biological activities in plants, such as the development of various organs and response to environmental stress (Liu et al. 2014; Liu et al. 2016). Arabidopsis has 12 RPD3/HDA1 members, some of which are known to be involved in development. For example, *HDA6* and *HDA19* are required for the repression of embryonic traits in post-embryonic development (Tanaka et al. 2008). In early leaf development, HDA6 represses *KNOX* genes by physically interacting with ASYMMETRIC LEAVES1 (AS1) to promote leaf differentiation (Luo et al. 2012). HDA9 also plays a role in controlling leaf size by promoting cell proliferation together with OLIGOCELLULA1/HIGH EXPRESSION OF OSMOTICALLY RESPONSIVE GENES15 (OLI1/HOS15) and POWERDRESS (PWR) (Chen et al. 2016; Kim et al. 2016; Suzuki et al. 2018). In the root, cellular patterning of the epidermis is affected in *hda6*, *hda18* and *hda19* mutants (Liu et al. 2013; Li et al. 2015). In addition, in *Zea mays* (maize), loss of function of HDA108 and downregulation of HDA101 lead to

various developmental defects in the shoots, leaves, and inflorescences (Rossi et al. 2007; Forestan et al. 2018).

In rice, the importance of histone acetylation has been demonstrated in a study showing that elevated levels of the histone acetyltransferase (HAT) gene enhance grain weight and yield (Song et al. 2015). However, the role of the HDAC genes in the development and morphogenesis of rice plants is poorly understood. An exception is *HDA702* (*OsHDAC1*), which has been shown to control seedling root growth by repressing *OsNAC6*; however, that result was obtained by overexpression analysis (Jang et al. 2003; Chung et al. 2009). To my knowledge, genetic analysis of HDAC genes using rice mutants has not been reported.

In this study, I isolated a rice mutant, named *dwarf with slender leaf 1* (*dsl1*), which showed pleiotropic defects in development, including narrow leaves, dwarfism, and small panicles. The narrow leaf phenotype was associated with both reduced vein numbers and narrower intervals between the veins. Both morphological analysis and expression analysis of cell cycle marker genes suggested that *DSL1* is involved in regulating cell proliferation to some extent. Gene cloning revealed that *DSL1* encodes an HDAC of the RPD3/HDA1 family that is closely related to Arabidopsis *HDA9* and *HDA6*. Consistent with the pleiotropic alterations observed in *dsl1*, expression of

DSL1 is ubiquitous. Taken together, my results suggest that an HDAC gene, *DSL1*, plays various roles in organ development in rice, similar to HDAC genes in Arabidopsis and maize.

Composition of this thesis

In this thesis, I aimed to isolate a novel gene that regulates rice development and to gain some insights to understand the molecular mechanism of rice development. In Chapter II, I show the results of the phenotypic analysis of *dsl1* and the functional analysis of *DSL1*. In Chapter III, I discussed the function of *DSL1* based on the results. In Chapter IV, I describe the materials and methods used in my study. Lastly, in Chapter V, I summarize this study and describe prospects in brief.

Chapter II

Results

The *dsl1* mutant has small leaves with a reduced number of vascular bundles.

To increase our understanding of rice development, I isolated a new mutant that showed semi-dwarfism and named it *dwarf with slender leaf1* (*dsl1*) (Fig. 1A, B). I first analyzed the *dsl1* mutant by focusing on leaf phenotypes. To assess the size of the leaves, I measured the 4th, 9th, 15th, and penultimate leaf (PN, formed just before the flag leaf), which represent early to late stages of vegetative growth. The results showed that the lengths of both the leaf blade and leaf sheath at each position were reduced in *dsl1* as compared with wild type (Fig. 1C; 2A, 2B).

Because the leaf width varies along the proximal–distal axis in the leaf blade, I measured the width at a fixed position, named the "fusion point" (Fig. 1B). The fusion point is defined as the position where the first large vein is fused to the midrib (Kubo et al. 2017). The results showed that the width of the leaf blade at this position in each leaf measured was significantly narrower in *dsl1* than in wild type (Fig. 1D). In rice, the longitudinal veins are arranged in parallel. I found that the number of both large and small veins were reduced in *dsl1*; in particular, the small veins were more prominently reduced (Fig. 1E, F).

Epidermal and inner tissues are affected by the *dsl1* mutation.

Next, to characterize the *dsl1* leaf at the tissue level, I performed histological analyses. First, I examined the distance between the small veins. To this end, the 9th leaf blades were cleared by the TOMEI-I method (Hasegawa et al. 2016) (Fig. 3A). I found that the distance between the small veins was significantly smaller in *dsl1* leaves than in wild-type leaves (Fig. 3A, E). Close examination of the inner tissues revealed that the number of cells between the small vascular bundles was reduced in *dsl1* (Fig. 3B, F). The distance between small vascular bundles was reduced about 0.83-fold in *dsl1*, while the number of cells between them was similarly reduced 0.83-fold. Thus, the narrower distance between the veins in *dsl1* seems to result from a reduction in cell number rather than cell size. Collectively, the narrow leaf blade width in *dsl1* is probably due to a reduction in both the number of the veins and the distance between them.

Histological observations also suggested that the size of vascular bundle was smaller in *dsl1* (Fig. 3B), an observation supported by measurement of the area of the small vascular bundle (Fig. 2C). Quantitative analysis showed that the smaller size of the vascular bundle resulted from a reduction in cell number (Fig. 3D, G). Thus, these analyses revealed that the *dsl1* mutation leads to fewer cells both in the region between

the small vascular bundles and in the small vascular bundles themselves.

Lastly, I compared the epidermal surface of the leaf blade between *dsl1* and wild type. The adaxial epidermis consisted of stomata cells and several other types of cell, which were distinguished by their shape and pattern of small distinctive protuberances (Fig. 3C). The cells with the distinctive protuberances were arranged in parallel and were associated with inner structures such as vascular bundles and bulliform cells (Fig. 3C, D). Although similar morphological features were observed in both wild-type and *dsl1* leaves, the number of cell files was significantly reduced in *dsl1* (Fig. 3H). In addition, the shapes of cells were also affected in *dsl1*. For example, the epidermal cells just above the vascular bundle had a simple contour in *dsl1* leaves as compared with a jigsaw piece-like shape with complex contours in wild-type leaves (Fig. 3C, insets).

Effect of the *dsl1* mutation on early leaf development.

Next, I assessed the effect of the *dsl1* mutation on an early stage of leaf development. I examined the spatial expression pattern of cyclin-dependent kinase B2 (*CDKB2*), a marker of G2/M phase in the cell cycle (Oikawa and Kyozuka 2009). Yasui et al. (2018) showed that *CDKB2* was a useful marker to examine the activity of leaf

primordia. In wild type, *CDKB2* was expressed in a patchy pattern from P1 to P4 (Fig. 4A) (For sense probe control, see Fig. 4F, G). In comparison, the expression levels of *CDKB2* were reduced in these leaf primordia in *dsl1* (Fig. 4B). In addition, the number of cells expressing *CDKB2* was also decreased in *dsl1* (Fig. 4B, E), suggesting that cell cycle progression was affected in this mutant.

Because leaf development is associated with SAM activity, I also examined the SAM in the *dsl1* mutant. To observe the SAM, I cleared the shoot apex of 29-day-old seedlings by using chloral hydrate solution. The SAM shape in *dsl1* differed slightly from that in wild type: *dsl1* had a rounder and flatter SAM, as compared with wild type (Fig. 4C, D). I confirmed this slight alteration of *dsl1* SAM shape by comparing eight shoot apices for both *dsl1* and wild type.

***dsl1* has a distinct pattern of internode elongation.**

As described above, the *dsl1* mutant showed dwarfism in the vegetative phase (Fig. 1A). I therefore assessed whether the internode length of the culm is affected by this mutation by examining the primary shoot after heading. The results showed that the lengths of three internodes (II, III and IV) were significantly shortened in *dsl1* as compared with wild type (Fig. 5A, B). The lengths of internodes I and V were mostly

comparable between wild type and *dsl1*. On the other hand, internode VI was not detected in 8 of 14 wild-type plants, whereas this internode was elongated in all *dsl1* plants examined (n=13) (Table 1; Fig. 5B, right panel). Furthermore, internode VII, which was invisible in wild type, was detected in 5 of 13 *dsl1* plants (Table 1). Thus, despite the overall dwarf phenotype, the elongation of lower internodes seems to be promoted in *dsl1*. To my knowledge, an internode phenotype similar to that observed in *dsl1* has not previously been reported.

The *dsl1* mutation affects inflorescence and spikelet morphology.

Next, I examined the inflorescence and spikelet phenotypes of *dsl1*. The rice inflorescence, called a panicle, consists of a rachis, branches, and spikelets (Fig. 6A). The *dsl1* panicle was apparently smaller than the wild-type panicle (Fig. 6B). Consistent with this observation, the length of the rachis and the primary branches were significantly reduced in *dsl1* as compared with wild type (Fig. 6K; 7A). In addition, the number of primary branches and the number of spikelets per branch was also decreased in *dsl1* (Fig. 6L, M). Collectively, these observations suggest that the activities of both the inflorescence and branch meristems are low in *dsl1*.

The width of the lemma and palea in *dsl1* spikelets was slightly slender as

compared with wild-type spikelets (Fig. 6E, F). Consistent with this observation, the seed width of *dsl1* was significantly narrower than that of wild type (Fig. 7D, E). At the top of the primary branches, I observed two types of abnormality, categorized as slight and severe. The slight type involved slender terminal spikelets, similar to most spikelets, as described above, although a markedly slender spikelet was observed on the uppermost primary branch (Fig. 6G). The severe type involved the formation of abnormal appendages instead of the terminal spikelet (Fig. 6H-J'). In some cases, the appendages were similar to sterile lemma or rudimentary glumes of the wild-type spikelet (Fig. 6H-I'). In another severe case, the branches were abruptly ended without any appendages (Fig. 6J, J'). These severe abnormalities were observed in about half of the primary branches. Overall, it seems that development of the terminal spikelets is markedly disturbed relative to the lateral spikelets in *dsl1*.

Even at the stage of seed maturation in wild type, the *dsl1* panicle was upright and the matured panicle was very light (Fig. 7B), suggesting that seed development was disturbed in *dsl1*. In fact, the fertility of *dsl1* was very low: only about 7% of the spikelets produced were filled with a sufficient amount of endosperm (Fig. 6N). Although the flowers were apparently normal, the anthers were pale yellow in *dsl1*, suggesting that pollen development was impaired (Fig. 7C). Observation of pollen

showed that many of the *dsl1* grains were contracted and appeared to be empty (Fig. 6C). In addition, the *dsl1* pollen grains showed less staining with I_2-KI, indicating no starch accumulation (Fig. 6D). Collectively, these observations suggest that low pollen viability is a major cause of the low fertility of *dsl1*.

DSL1 encodes a histone deacetylase

To isolate the gene responsible for the *dsl1* mutant, I performed positional cloning. I crossed *dsl1* with Kasalath, an *indica* strain, and selected rice plants exhibiting narrow leaves from the F_2 plants. Using these plants, I roughly mapped the *DSL1* locus to a region between 19.736 and 20.439 Mb on chromosome 4 (Fig. 8A). Next, I determined the whole sequence of the *dsl1* genome by Illumina sequencing technology, and found that three genes (Os04g0400700, Os04g0407800, Os04g0409600) had a mutation related to protein function as compared with the reference genome, Nipponbare. Next, I found that Kinmaze, the genetic background of *dsl1*, had the same mutation as *dsl1* in Os04g0400700 and Os04g0407800, suggesting that Os04g0409600 (LOC_Os04g33480) is likely to be the candidate gene for *DSL1*. A similarity search indicated that the candidate gene for *DSL1* is a member of the RPD3/HDA1 family (Pandey et al. 2002; Fu et al. 2007), and that

Os04g0409600 in the *dsl1* mutant has a missense mutation in the sequence corresponding to an HDAC domain (Fig. 8B) (see below in detail).

To confirm that *DSL1* is Os04g0409600, I disrupted Os04g0409600 by using CRISPR-Cas9 (clustered regularly interspaced short palindromic repeats-CRISPR-associated protein 9) genome editing technology and analyzed the resulting phenotypes (Fig. 8B; 9). Os04g0409600 knockout lines were generated in Taichung 65 (T65) because the transformation efficiency of Kinmaze is known to be low. Subsequently, I analyzed two regenerated plants with biallelic mutations in Os04g0409600 (R38 and R48) in addition to descendants of a regenerated plant with a monoallelic mutation (R19).

The R38 and R48 plants had biallelic loss-of-function mutations including a frame-shift and 34-bp deletion (Fig. 9B). Both plants showed a semi-dwarf phenotype, as compared with a regenerated plant that had no mutation in Os04g0409600 (Fig. 10A). The R38 and R48 plants also showed other *dsl1*-like characteristics, such as narrow leaves, a reduced interval between vascular bundles, and abnormal inflorescences (Fig. 8C; 10B-D).

Next, I examined next-generation plants produced by self-pollination of the R19 plant, which had a 34-bp deletion loss-of-function allele and a wild-type allele.

The plants that were homozygous for the mutant allele showed phenotypes similar to those observed in the *dsl1* mutant, whereas both heterozygous plants and those homozygous for the wild-type allele were similar to wild type (Table 2). The phenotypes of the homozygous mutant descendants included narrower intervals between small vascular bundles, small inflorescences, and narrow spikelets (Fig. 8C; 10D, E). The phenotypes and genotypes of these descendants showed complete agreement with each other (Table 2). Thus, pleiotropic defects, which are seldom observed in a single recessive mutant of general developmental genes, were observed in common between the *dsl1* mutant and plants homozygous for mutant alleles of Os04g0409600. From these results, I concluded that the *DSL1* gene is Os04g0409600. Hereafter, I refer to Os04g0409600 as *DSL1*.

DSL1 is a class I member of the RPD3/HDA1 family

As described above briefly, *DSL1* encodes a histone deacetylase (HDAC) belonging to the RPD3/HDA1 family. Rice has 14 members in this family, whereas Arabidopsis has 12 members. I constructed a phylogenetic tree of the genes in rice, Arabidopsis and maize (Fig. 11A), after excluding genes with an incomplete HDAC domain (see Materials and Methods), which showed that RPD3/HDA1 family members are

classified into several classes, as previously described (Pandey et al. 2002; Fu et al. 2007). I found that *DSL1* belongs to class I and is closely related to Arabidopsis *HDA6* and *HDA9* (Fig. 7A) (Liu et al. 2014; Liu et al. 2016). Although Os04g0409600 was temporally named HDA711 in previous sequence studies (Pandey et al. 2002; Fu et al. 2007), its function has remained unknown. Sequence comparison of the HDAC domain showed that the missense mutation in *dsl1* occurs at an amino acid that is invariant among the class I HDACs (Fig. 11B).

Next, I examined organ-specific expression of *DSL1* in wild type. In RT-PCR analysis, *DSL1* was expressed in the leaf blade and leaf sheath at all growth stages examined. In addition, *DSL1* expression was detected in developing inflorescences, spikelets, and roots (Fig. 11C). This ubiquitous expression is consistent with the observation that the *dsl1* mutant shows various defects in the vegetative and reproductive phase.

Lastly, I performed microarray analysis using shoot apices including the SAM and P1–P4 primordia and extracted genes that were differentially expressed between *dsl1* and wild type by the rank product method (FDR<0.05) (Breitling et al. 2004). However, the number of extracted genes was very small: the number of up-regulated genes in *dsl1* was 134, whereas that of down-regulated genes was 45. This small

change in gene expression profile in *dsl1* is likely to result from genetic redundancy among the HDAC genes. Furthermore, the expression levels of known genes associated with leaf morphology, such as *NAL2/3* and *NAL7*, did not show significant differences between *dsl1* and wild type (Fig. 12).

Gene ontology (GO) enrichment analysis found that only three GO terms including response to stimulus and stress (GO:0050869, GO:0006950, and GO:0009607 [agriGO v2.0, Tian et al. 2017; http://systemsbiology.cau.edu.cn/agriGOv2/]) were enriched among the up-regulated genes (Table 3). No GO term was enriched among the down-regulated genes. In general, HDAC genes are known to be involved in regulating the response to environmental changes (Liu et al. 2014; Liu et al. 2016). Therefore, the enrichment of these GO terms suggests that the function of *DSL1* might be also associated with environmental response.

Table 1. Number of plants elongating each internode.

internode	IV	V	VI	VII	
WT	14	14	6	0	(n=14)
dsl1	13	13	13	5	(n=13)

Table 2. Genotypes and phenotypes in the descendants of R19 plants heterozygous for *dsl1*.

No of descendant	4	6	10	11	12	13	14	16	17	18
genotype	*W/m*	*m/m*	*m/m*	*W/m*	*W/W*	*W/W*	*W/m*	*W/W*	*m/m*	*W/m*
Dwarfism	no	yes	yes	no	no	no	no	no	yes	no
Slender leaf	no	yes	yes	no	no	no	no	no	yes	no
Spikelet defects	no	yes	yes	no	no	no	no	no	yes	no

W, wild-type allele; *m*, mutant allele

Table 3. GO terms enriched among the up-regulated genes in *dsl1*.

GO accession number	GO term	queryitem	querytotal	bgitem	bgtotal	pvalue	FDR
GO:0050896	response to stimulus	53	120	6928	34296	2.80E-09	4.50E-07
GO:0006950	response to stress	41	120	4660	34296	9.60E-09	7.70E-07
GO:0009607	response to biotic stimulus	19	120	1404	34296	5.00E-07	2.70E-05

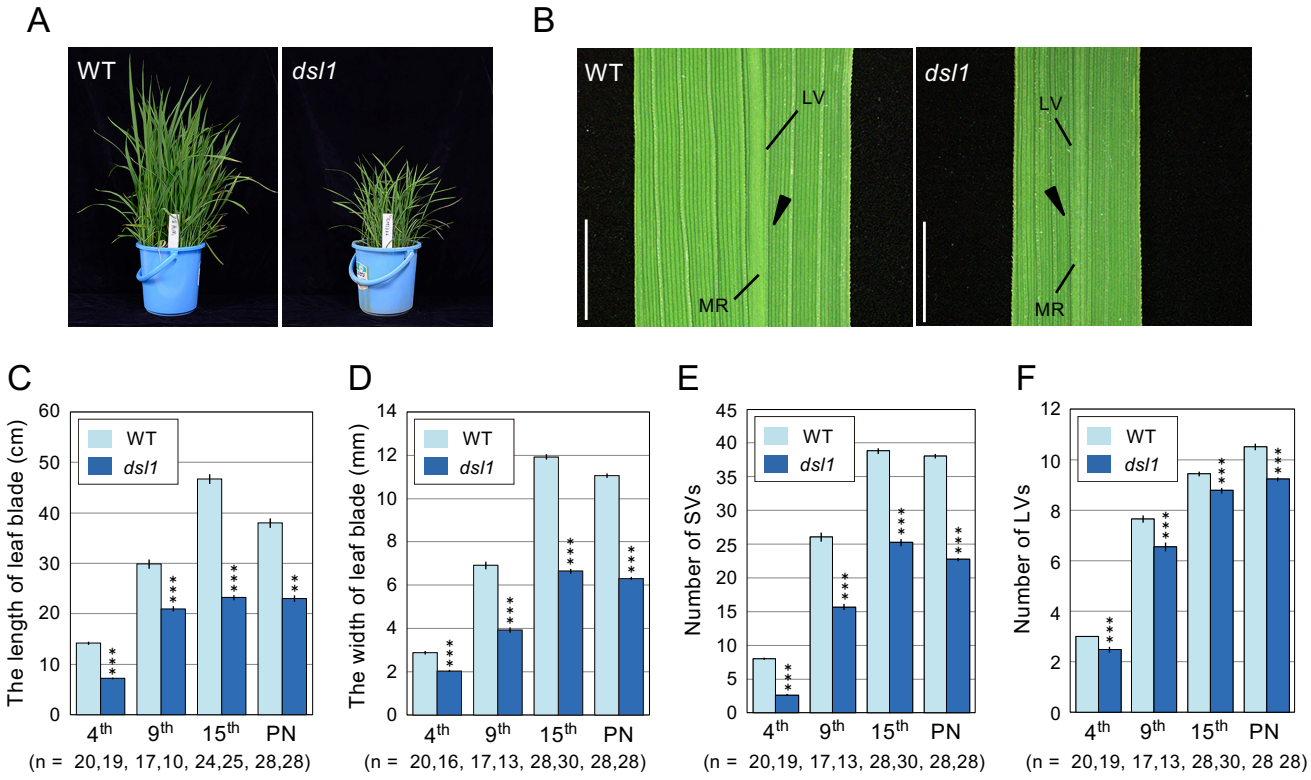

Fig. 1 Phenotypes of leaves in wild type and the *dsl1* mutant.

(A) Pot-grown 68-day-old plants.

(B) Adaxial sides of the 15th leaf blades. Arrowheads indicate the "fusion point."

(C) Length of leaf blade.

(D) Width of leaf blade.

(E) Number of small veins.

(F) Number of large veins.

LV, large vein; MR, midrib; SV, small vein; PN, penultimate.

Asterisks (C-F) indicate statistically significant differences between WT and *dsl1* by Student's t-test. Error bars represent SE. **p<0.01, ***p<0.001.

Scale bars = 5 mm (B).

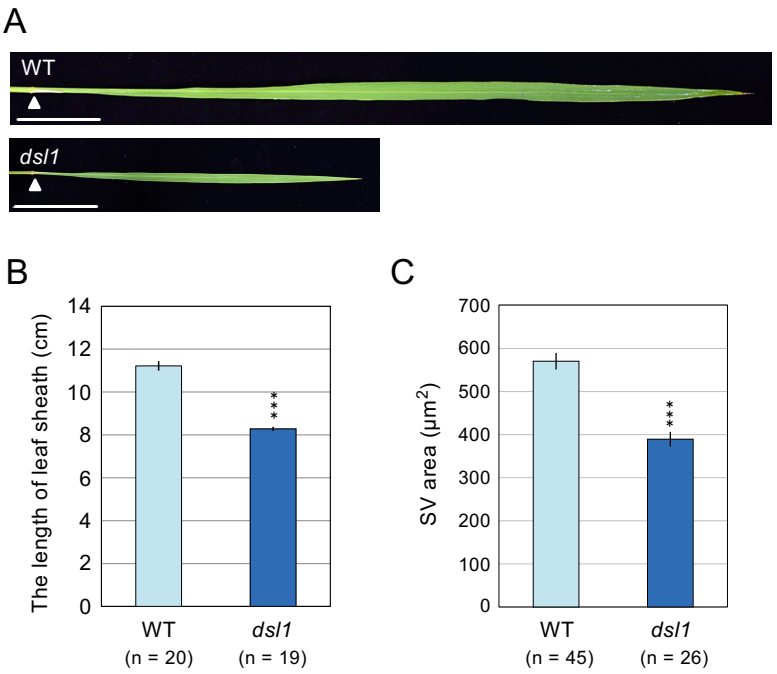

Fig. 2 Phenotype of wild-type and *dsl1* leaves.
(A) Whole images of the 15th leaf blade. White arrowheads indicate the lamina joint. Scale bars = 5 cm.
(B) Length of the 4th leaf sheath.
(C) Area of the small vascular bundle in the 9th leaf blade.
Asterisks (B,C) indicate statistically significant differences between WT and *dsl1* by Student's t-test. Error bars represent SE. ***p<0.001.

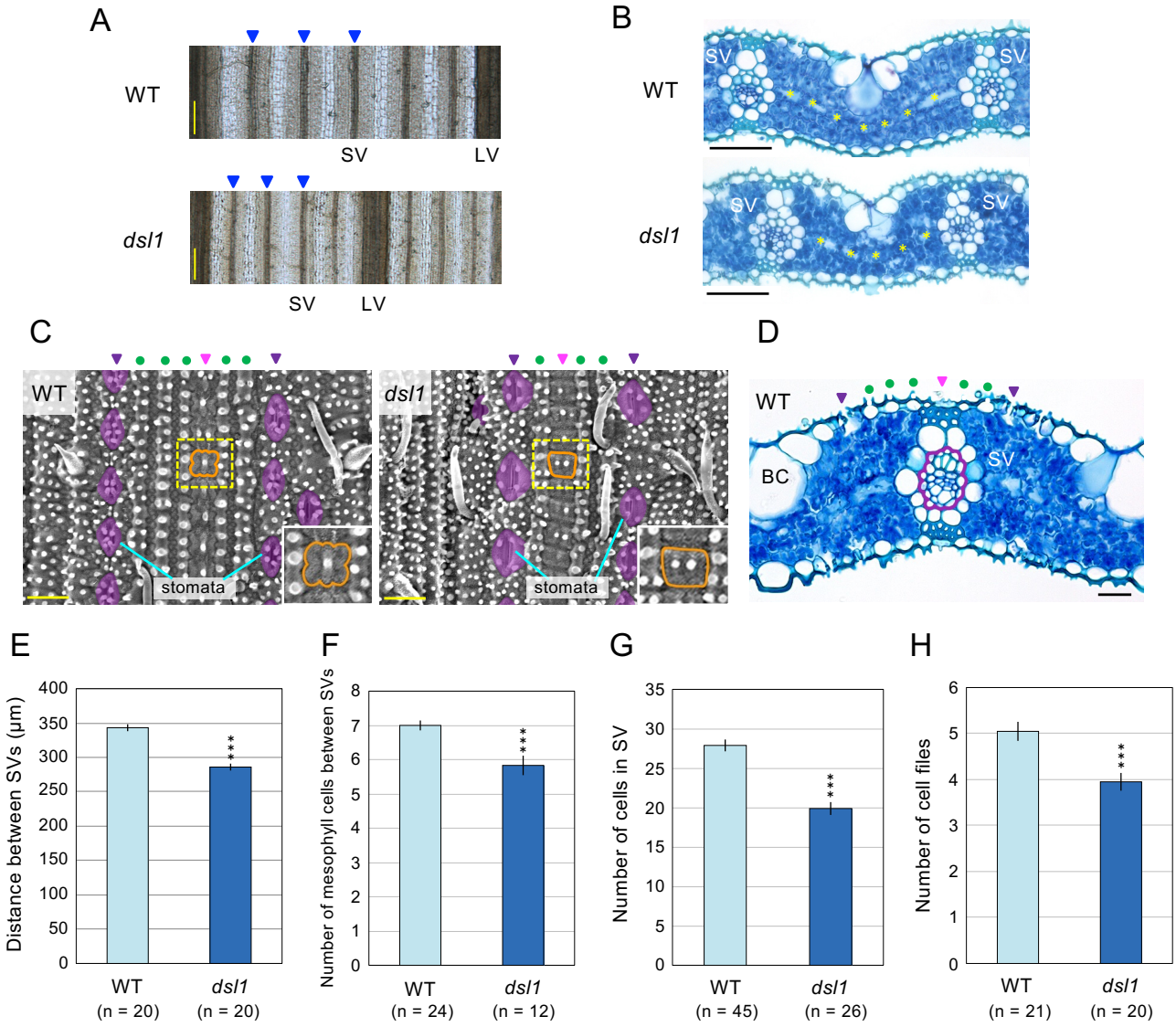

Fig. 3 Histological analysis of the leaf blade of wild type and *dsl1*.

(A) Leaf blades (9th) cleared by the TOMEI-I method.

(B) Transverse sections of leaf blades (9th) around the "fusion point." Cells marked with yellow asterisks (B) were counted in (F).

(C) SEM images of the adaxial epidermis of the leaf blades (15th). Insets show magnification of the regions in the yellow boxes (an epidermal cell shape is outlined with an orange line). Purple arrowheads and areas indicate stomata complex and their cell files, respectively.

Pink arrowheads indicate epidermal cells just above the vascular bundle. Cell files with green dots were counted in (H).

(D) Transverse section of wild-type leaf blade (15th) around the "fusion point."

The purple line delineates the region where the cell number and area of the small vein were measured (G and Fig. 2C).

(E) Distance between small veins in the 9th leaf.

(F) Number of mesophyll cells (yellow asterisks in (B)) between the small veins in the 9th leaf.

(G) Number of cells in the small veins in the 9th leaf (D).

(H) Number of cell files (indicated with green dots in (C)) in the 15th leaf. BC, bulliform cell; SV, small vein (A) and small vascular bundle (B, C); LV, large vein.

Asterisks (E-H) indicate statistically significant differences between WT and *dsl1* by Student's t-test. Error bars represent SE. ***$p<0.001$.

Scale bars = 100 μm (A), 50 μm (B), and 20 μm (C, D).

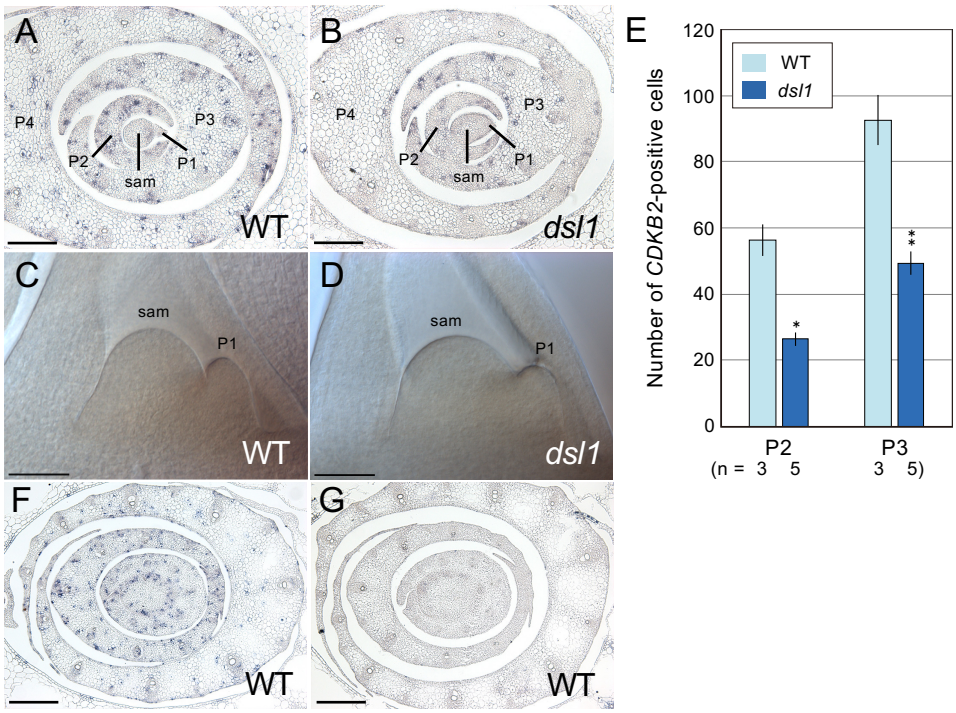

Fig. 4 Shoot apices with the SAM and leaf primordia in wild type and *dsl1*.
(A, B) Cross-section showing spatial expression pattern of *CDKB2* (2-week-old plants).
(C, D) Shoot apices cleared by chloral hydrate solution. sam, shoot apical meristem.
(E) The number of *CDKB2*-positive cells.
(F, G) Negative control of the in situ hybridization of *CDKB2*. (F) *CDKB2* antisense probe. (G) *CDKB2* sense probe. The shoot apices of 2-weeks-old wild-type plants (Kinmaze) were used.
sam, shoot apical meristem. P, plastchron.
Asterisks (E) indicate statistically significant differences between WT and *dsl1* by Student's t-test. Error bars represent SE. *$p<0.05$, **$p<0.01$.
Scale bars = 200 μm (A, B, F, G) and 50 μm (C, D).

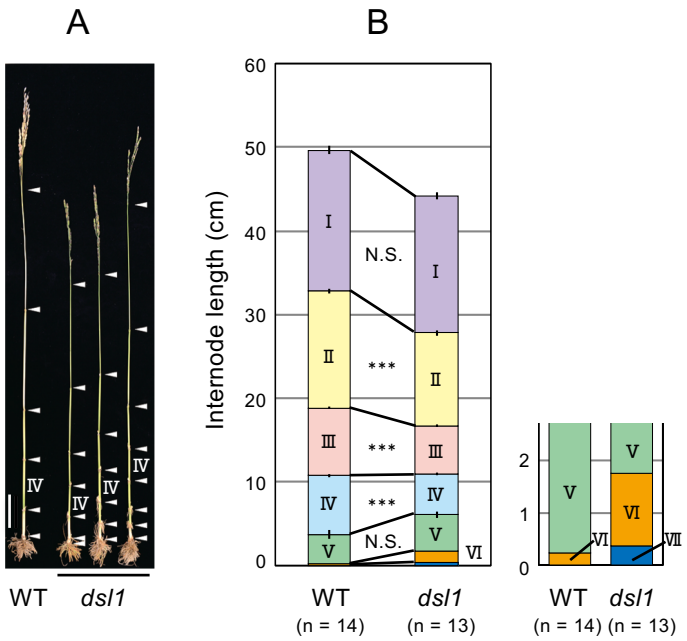

Fig. 5 Internodes of wild type and *dsl1*.
(A) Whole images of the main culm. White arrowheads indicate nodes. Scale bar = 5 cm.
(B) Comparison of the lengths of each internode. The graph on the right shows a magnification of the lower part of that on the left to compare internodes VI and VII.
Asterisks (B) indicate statistically significant differences between WT and *dsl1* by Student's t-test. Error bars represent SE. N.S., Not Significant. ***p<0.001.

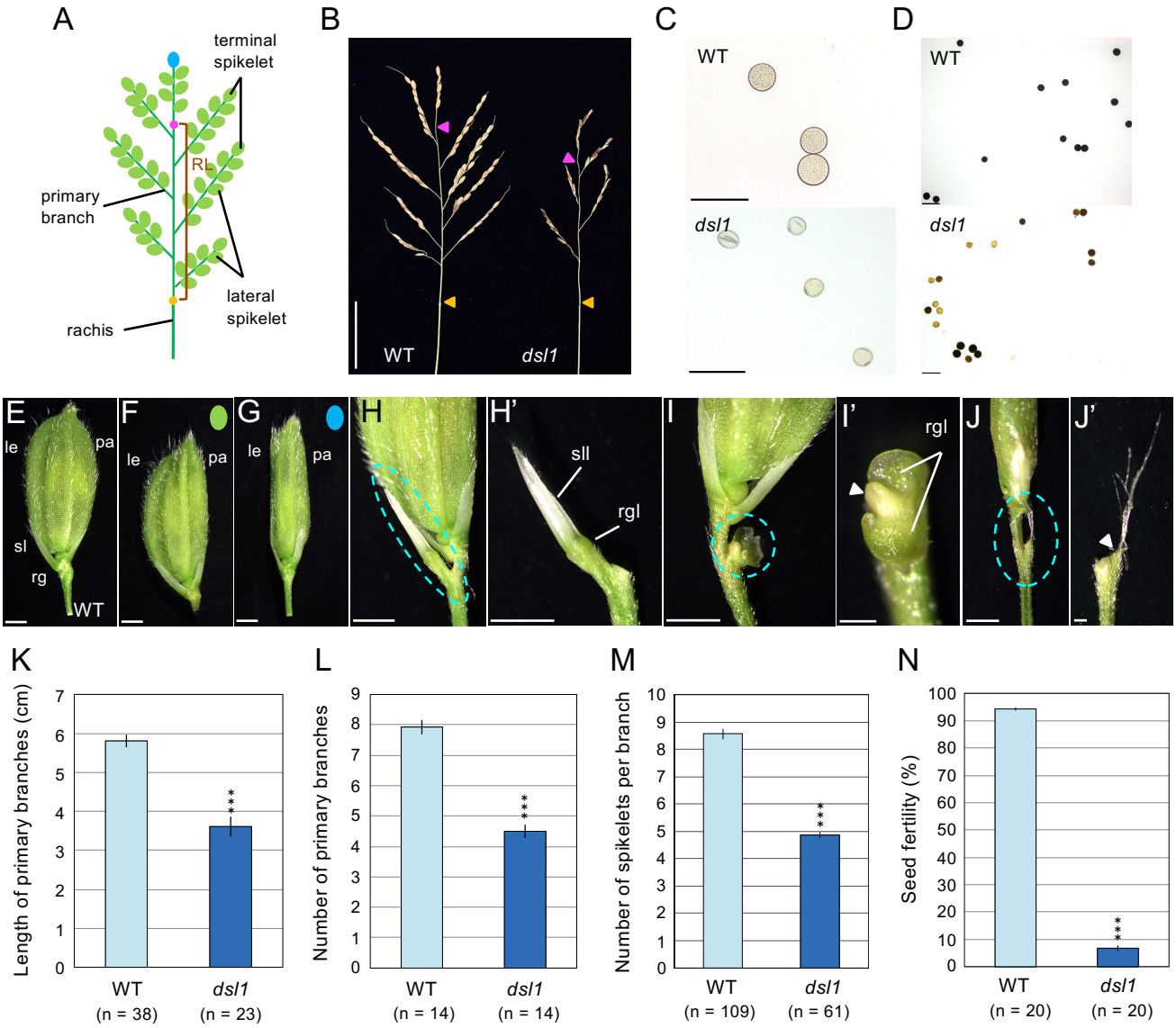

Fig. 6 Phenotypes of inflorescences and spikelets in wild type and *dsl*1.

(A) Schematic diagram of a rice inflorescence. Magenta and orange dots indicate the remnant of the inflorescence meristem and the panicle bract, respectively.

(B) Inflorescence of wild type and *dsl1*. Magenta and orange arrowheads indicate the remnant of the inflorescence meristem and the panicle bract, respectively.

(C) Pollen grains of WT and *dsl1*.

(D) I_2-KI staining of pollen grains of WT and *dsl1*.

(E) A wild-type spikelet.

(F, G) A *dsl1* spikelet. The position of the spikelets in (F) and (G) are indicated by the respective green and blue circles in (A).

(H-J, H'-J') Appendages generated at the top of the primary branches. (H'-J') are magnifications of the region within the cyan broken line in (H-J). Arrowheads (I' and J') indicate abruptly ended primary branches.

(K) The length of primary branches.

(L) Number of primary branches.

(M) Number of spikelets per branch.

(N) Seed fertility. le, lemma, pa, palea; rg, rudimentary glume, rgl, rudimentary glume-like organ; RL, rachis length; sl, sterile lemma; sll, sterile lemma-like organ.

Asterisks (K-N) indicate statistically significant differences between WT and *dsl1* by Student's t-test. Error bars represent SE. ***p<0.001.

Scale bars = 5 cm (B), 100 μm (C, D), 1 mm (E-J, H'), and 250 μm (I', J').

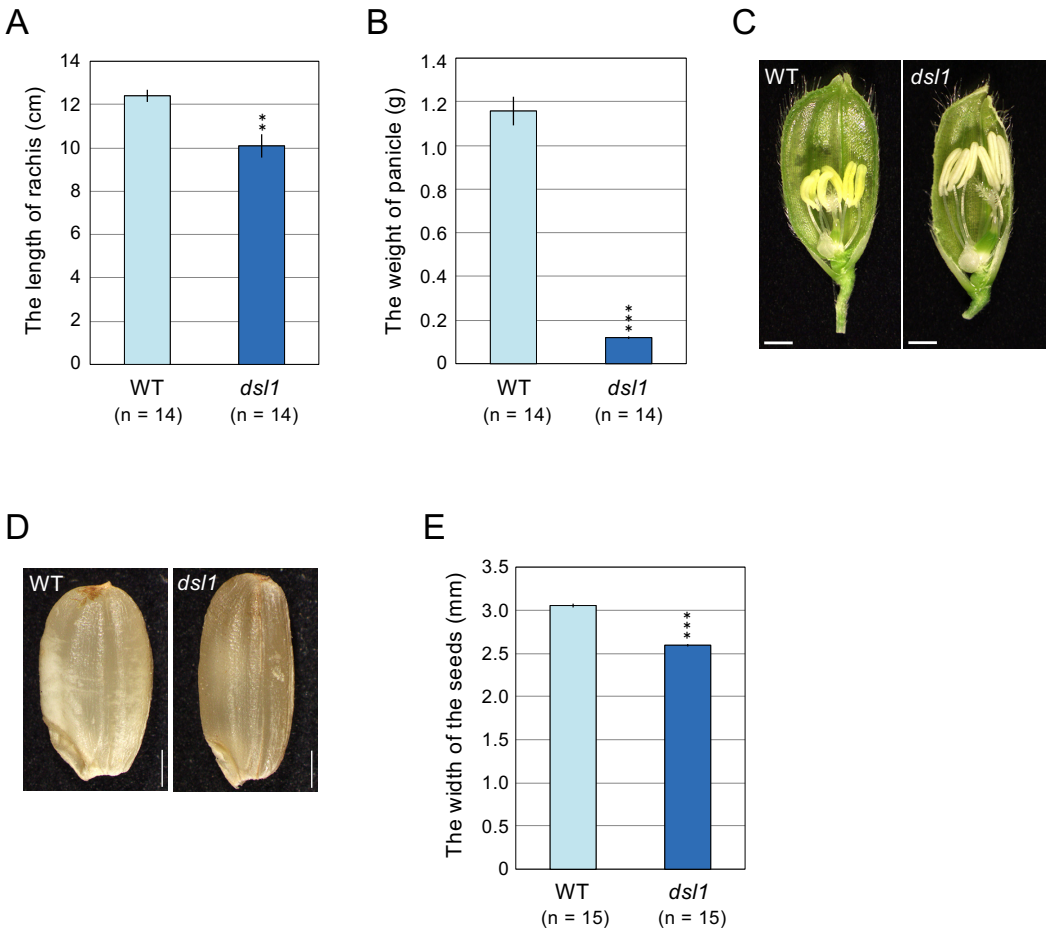

Fig. 7 Phenotypes of inflorescences and spikelets in wild type and *dsl1*.
(A) Length of the rachis.
(B) Weight of the panicle.
(C) Inner structure of the spikelet.
(D) Wild-type and *dsl1* seeds.
(E) Width of the seeds.
Asterisks (A,B,E) indicate statistically significant differences between WT and *dsl1* by Student's t-test. Error bars represent SE. **p<0.01; ***p<0.001.
Scale bars = 1 mm (C, D).

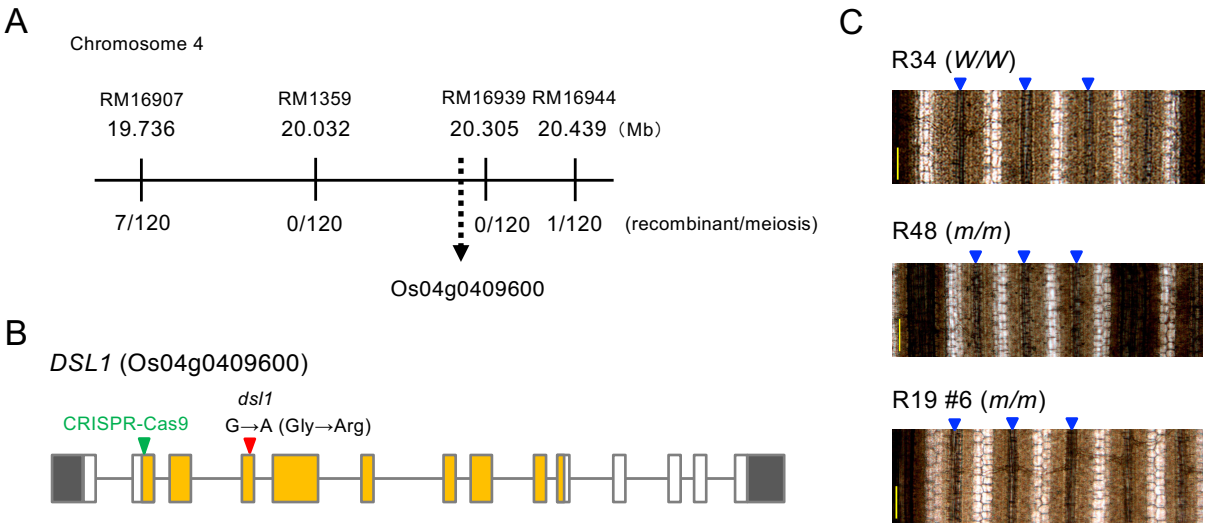

Fig. 8 Identification of the *DSL1* gene.
(A) Position of the *DSL1* locus on chromosome 4.
(B) Schematic representation of *DSL1*. The mutation site in *dsl1* and the position of the targeted disruption by CRISPR-Cas9 are indicated by red and green arrowheads, respectively. Boxes and solid lines indicate exons and introns/flanking regions, respectively. Orange boxes correspond to the HDAC domain.
(C) Leaf blades (PN) cleared by the TOMEI-I method. R34 is homozygous for wild-type *DSL1*. R48 and R19 #6 (a next-generation plant of R19) has biallelic loss-of-function mutations in *DSL1*.
Scale bars = 100 μm.

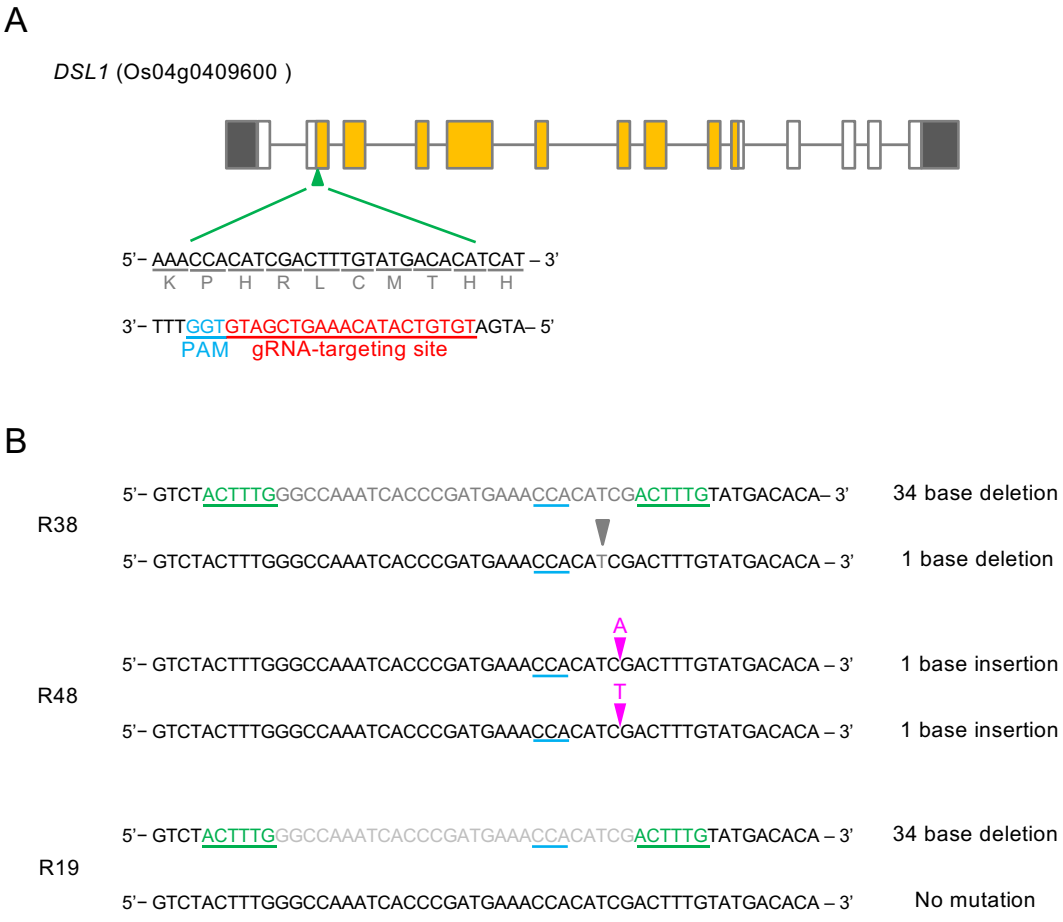

Fig. 9 Mutations generated by CRISPR-Cas9 technology.
(A) Target sequence for disruption of *DSL1* (Os04g0409600).
(B) Sequences of the *DSL1* gene in knockout lines. Blue underlining indicates the PAM sequence, magenta arrowheads indicate nucleotide insertions, and gray letters indicate a deleted nucleotide (gray arrowhead) or deleted sequence. The deleted region contains two repeated short sequences, ACTTTG (green letters); one of these sequences is deleted in lines R38 and R19.

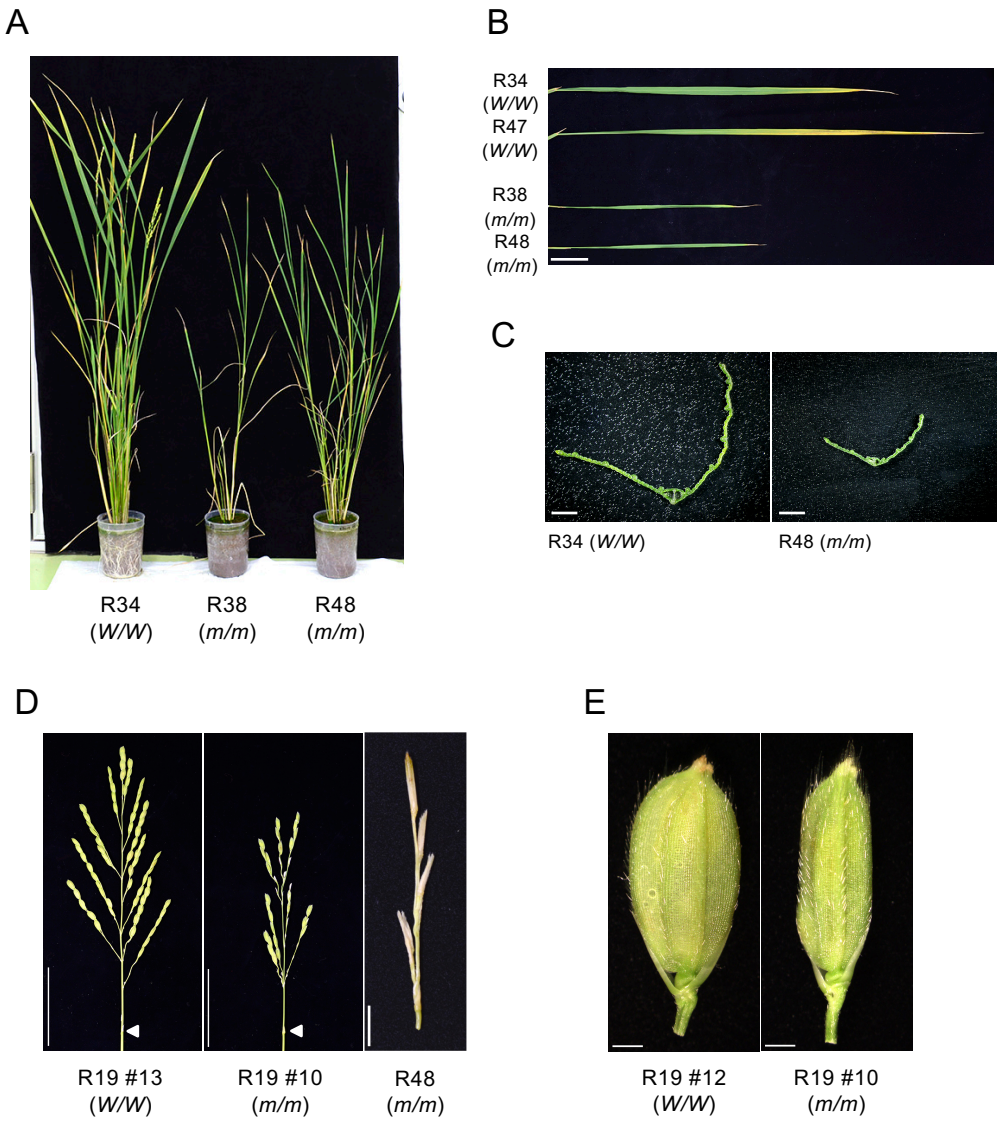

Fig. 10 Phenotypes of leaves, inflorescences, and spikelets in the mutants generated by CRISPR-Cas9 technology.

(A) Transgenic plants at about 6 months after regeneration.

(B) Leaf blades (penultimate leaf).

(C) Cross-sections of the leaf blade around the "fusion point."

(D) Inflorescences.

(E) Spikelets.

W, wild-type allele; *m*, mutant allele.

Scale bars = 5 cm (B, R19#13 and R19 #10 in D), 5 mm (R48 in D), and 1 mm (C, E).

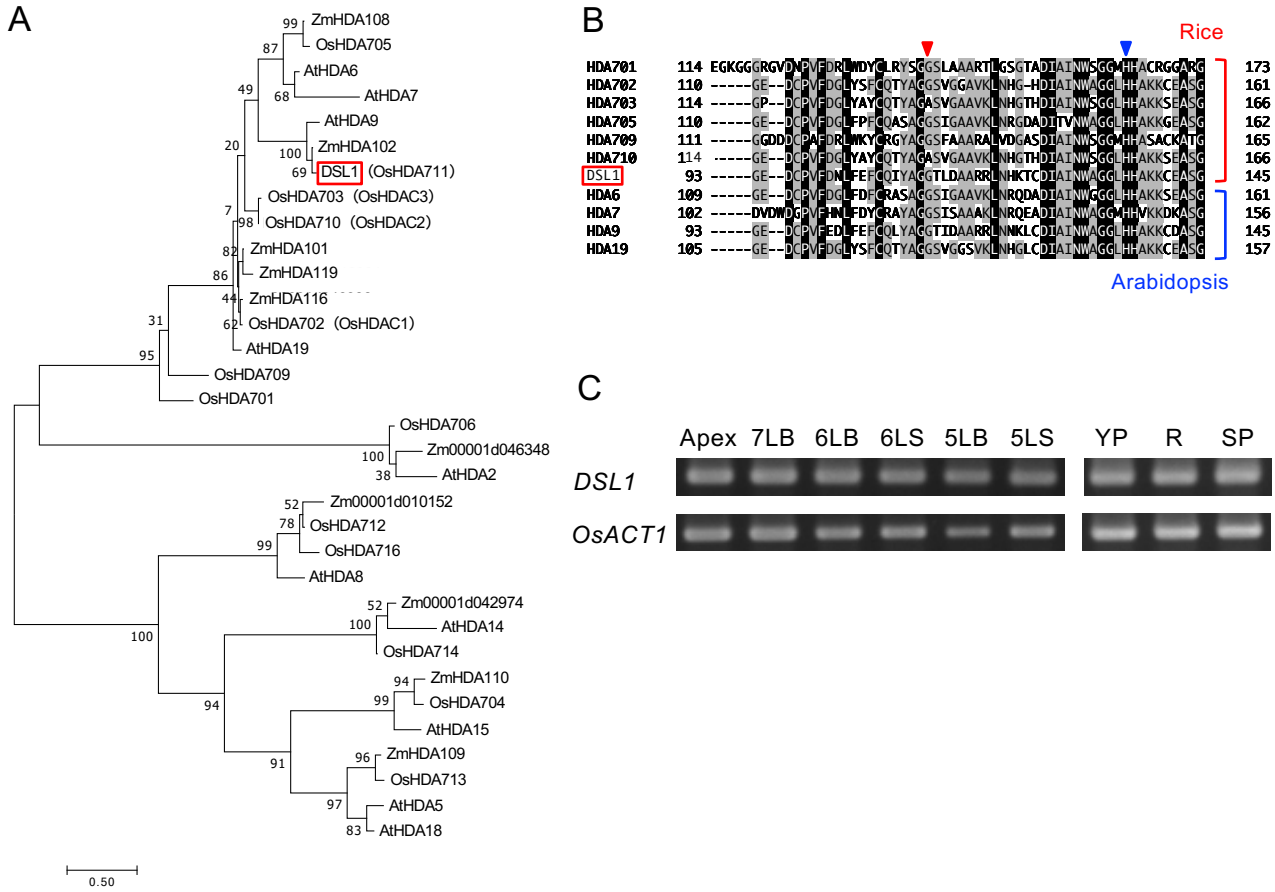

Fig. 11 Characterization of *DSL1*.

(A) Phylogenetic tree of HDACs in the RPD3/HDA1-like family. The tree was constructed by the maximum likelihood method using the sequences of the HDAC domain. Numbers above the branches indicate the bootstrap values calculated from 1000 replicates.

(B) Comparison of amino acid sequences in part of the HDAC domain. Red and blue arrowheads indicate, respectively, the mutation site of *dsl1* and the histidine related to the catalytic activity of HDAC.

(C) RT-PCR analysis of *DSL1* mRNA expression. The *ACTIN1* gene (*OsACT1*) was used as a control. Apex, shoot apex; 7LB, 7th leaf blade (P4 primordium); 6LB, 6th leaf blade; 6LS, 6th leaf sheath; 5LB, 5th leaf blade; 5LS, 5th leaf sheath; YP, young panicle (developing inflorescences, 3-8mm); R, root (5 days-old-plant); SP, spikelets just before heading.

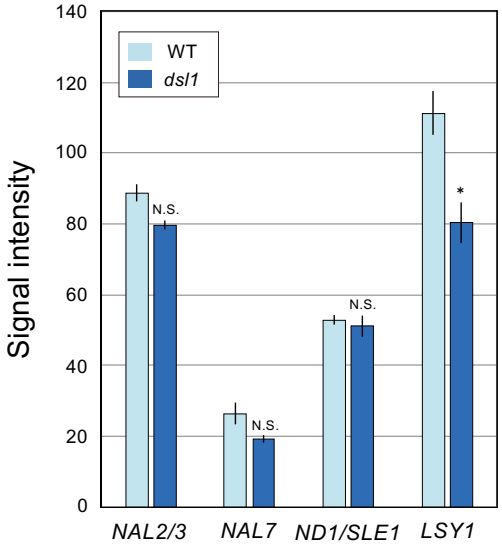

Fig. 12 Comparison of the expression levels of genes related to leaf development between *dsl1* and wild type.
Asterisk indicates statistically significant differences between WT and *dsl1* by Student's t-test. Error bars represent SE. N.S., Not Significant. *$p<0.05$.

Chapter III

Discussion

Pleiotropic phenotypes in the *dsl1* mutant result from defects in an HDAC gene

In this study, I showed that the *dsl1* mutant exhibited pleiotropic phenotypes in both the vegetative and reproductive phase. The pleiotropic phenotypes included slender leaves with a reduced number of veins, dwarfism with shorter internodes, small panicles with partially abnormal spikelets, and pollen sterility. A combination of mapping and next-generation sequencing revealed that *DSL1* (Os04g0409600) encodes an HDAC belonging to the RPD3/HDA1 family. Knockout lines of *DSL1* exhibited pleiotropic phenotypes similar to the *dsl1* mutant throughout the vegetative and reproductive phase, supporting the results of map-based gene identification.

DSL1 is a class I member of the RPD3/HDA1 family (Pandey et al. 2002; Fu et al. 2007). Although there are several reports of sequence and expression analyses, the function of genes in this family remains almost undocumented in rice. RNA silencing and overexpression of rice HDAC genes have been performed in a few studies, but developmental analysis is poor (Jang et al. 2003; Fu et al. 2007; Chung et al. 2009; Hu et al. 2009). This thesis, to my knowledge, is the first to show that an HDAC gene, *DSL1*, plays important roles in rice development through the characterization of

several independent mutant lines showing similar morphological defects.

Acetylation of histone relaxes the chromatin structure and is associated with transcriptional activation (Kadosh and Struhl 1998; Rundlett et al. 1998). HDACs remove this histone modification, leading to suppression of the target gene. Thus, HDACs are involved in chromatin-based gene regulation. During plant development, many genes must be regulated temporally and spatially in an appropriate manner, and genes that are unnecessary in a developmental process should be silenced at the chromatin level. Errors in gene silencing result in various developmental defects. For example, a dominant-negative mutation of the *TPL* gene encoding a Groucho/Tup1 family transcriptional corepressor causes the transformation of shoots into roots in the Arabidopsis embryo (Long et al. 2006). This type of transcriptional corepressor is generally known to recruit HDACs to the target site, and HDA19 has been shown to act together with TPLs (Long et al. 2006; Liu and Karmarkar 2008). Thus, HDACs play crucial roles in plant development.

Considering the general function of HDAC, the *dsl1* mutant seems to fail to repress a large number of genes that are silenced in wild type. Therefore, the pleiotropic phenotypes observed in this mutant are likely to result from spatial and temporal misexpression of a wide range of genes associated with rice development.

Although the *dsl1* mutation is pleiotropic, some phenotypes were weak. This may be associated with redundancy among the genes encoding HDACs, which constitute a multigene family (Pandey et al. 2002; Fu et al. 2007; Alinsug et al. 2009; Liu et al. 2016). This inference is consistent with my observation of only a small difference in gene expression profile between *dsl1* and wild type.

dsl1 exhibits pleiotropic defects in leaf development

My phenotypic analysis revealed that the *dsl1* mutant has pleiotropic defects in vegetative development. The *dsl1* leaves showed various defects, such as a reduction in size, a decrease in vein numbers, a shorter distance between veins, and altered epidermal morphology.

The narrow leaf phenotype was associated with a reduction of vein numbers in *dsl1*, similar to other narrow leaf mutants of rice. The patterns of reduction in the numbers of the large and small veins in the leaf blade are characteristic to each type of mutant. For example, the number of small veins is predominantly decreased in the *nal2 nal3* double mutant, whereas that of the large vein is almost unchanged (Cho et al. 2013; Ishiwata et al. 2013). By contrast, the mutation in *NAL7/COW1* causes a mostly equal reduction in the numbers of small and large veins (Woo et al. 2007;

Fujino et al. 2008; Kubo et al. 2017). In *dsl1*, the numbers of both veins were affected, although the reduction in the number of small veins was more evident.

Despite a reduction in vein numbers, the distance between the veins is unaffected in the *nal7/cow1* and *nal2 nal3* mutant. By contrast, a reduced distance between the small vascular bundles was observed in *dsl1*. My study showed that this reduced distance is associated with a decreased number of mesophyll cells and epidermal cell files. The number of cells in the vascular bundle itself was also reduced in *dsl1*, resulting in a reduction in its size. In addition, spatial expression analysis showed that *CDKB2* transcripts were reduced in the leaf primordia of *dsl1*. Collectively, these findings suggest that *DSL1* participates in regulating cell division and cell proliferation. Several genes responsible for narrow leaf mutants have been previously suggested to be involved in cell proliferation. For example, overexpression of *NAL2/3*, encoding a WOX-type homeodomain transcription factor, leads to an increase in small vein number and an expansion of leaf width (Ishiwata et al. 2013). The *sle1/nd1* gene encoding cellulose synthase-like protein D4 has also been shown to be associated with cell cycle progression (Li et al. 2009; Yoshikawa et al. 2013).

Overall, the finding that *dsl1* shows various defects in leaf morphology suggests that, as an HDAC, DSL1 is involved in regulating multiple genes responsible for leaf

development.

The *dsl1* mutation affects various morphological features in the reproductive phase

The *dsl1* mutant showed dwarfism. In the vegetative phase when no stem elongates, the apparent dwarf phenotype of *dsl1* seemed to result from the reduced length of both the leaf blade and sheath. The culm elongates after floral induction in rice. In the reproductive phase, the *dsl1* mutant also showed a dwarf phenotype, in which the culm was shorter as compared with wild type. The culm consists of several internodes. Takeda (1977) classified rice dwarf mutants into six types by the elongation pattern of each internode. For example, the second and third internodes are shortened in d6-type mutants, whereas only the second internode is shortened in dm-type mutants. In the *dsl1* mutant, three internodes (II, III, IV) were shortened; however, internode VI, which is very short in wild type, was slightly elongated. Notably, internode VII, which was not observed in wild-type plants of Kinmaze, was clearly observed in *dsl1*. Thus, the internode pattern of *dsl1* is unique, and has not been found in other rice dwarf mutants to my knowledge. The *d6* mutant, which is a d6 type, is defective in a gene encoding a KNOX-type homeodomain transcription factor (Sato et al. 1999), whereas

the *d61* mutant, which is a dm type, has a mutation in brassinosteroid biosynthesis (Yamamuro et al. 2000). Thus, various genes seem to be involved in regulating internode elongation. The unique internode patterning observed in *dsl1* suggests that *DSL1* may be involved in the elongation or suppression of culm internodes by controlling genes with diverse function.

The *dsl1* mutant generated small inflorescences and abnormal spikelets. The reduction in primary branch number and spikelet number per branch is likely to be associated with partially reduced activity of the inflorescence and branch meristems. The severe type of the abnormal spikelets seemed to result from developmental arrest at an early stage because they contained only a few spikelet organs. Furthermore, because the abnormal spikelets were detected only at the position of the terminal spikelets, and not at the lateral spikelets, the developmental arrest of the spikelets might be associated with a defect in conversion from the branch meristem to the spikelet meristem. Small inflorescences with a reduced number of primary branches and arrested spikelets, similar to those observed in *dsl1*, have also been found in the *asp1* mutant (Yoshida et al. 2012). *ASP1* encodes a transcriptional corepressor similar to TPL of the Groucho/Tup1 family (Yoshida et al. 2012). As described above, HDACs are recruited to their target site by a Groucho/Tup1 family corepressor (Liu

and Karmarkar 2008). Therefore, the similarity in defects observed in the *dsl1* and *asp1* mutants seems to be consistent with the related functions of the proteins encoded by the two genes. However, the frequency of abnormal spikelets observed in *dsl1* was lower than that reported in *asp1*, and was restricted to the terminal spikelets. In addition, elongation of the sterile lemma, a typical phenotype of *asp1* spikelets, was not observed in *dsl1*. These differences may be associated with the presence of multiple HDAC genes in the RPD3/HDA1 family.

The function of HDAC genes in plant development

In *Arabidopsis*, HDAC genes in the RPD3/HDA1 family are required for various developmental processes, such as embryogenesis, leaf and root development, and flowering, in addition to the response to environmental stress (Tanaka et al, 2007; Luo, 2012; Liu et al. 2014; Chen et al. 2016; Kim et al. 2016; Liu et al. 2016; Suzuki et al. 2018). Similarly, HDAC genes also play a role in development and morphogenesis by controlling the epigenetic status of various genes (Rossi et al. 2007; Forestan et al. 2018). In both *Arabidopsis* and maize, HDAC genes are expressed ubiquitously in various organs and tissues. Taking account into my findings on *DSL1*, the function of class I HDAC genes seems to be conserved in both monocots and eudicots.

Despite this general conservation, the function of *DSL1* is likely to be more similar to that of maize HDAC genes: rice *dsl1* and maize *hda108* display severe pleiotropic defects, such as reduced leaf size, dwarfism, and abnormal small inflorescences, as compared with Arabidopsis *hda6* and *hda9* (Luo et al., 2012; Li et al. 2015; Chen et al. 2016; Kim et al. 2016; Suzuki et al. 2018; Forestan et al. 2018). In particular, strong male sterility is observed in both rice *dsl1* and maize *hda108* mutants, but not in the corresponding Arabidopsis mutant. Although I failed to identify genes associated with the morphological phenotypes by microarray analysis owing to genetic redundancy, Forestan et al. (2018) successfully identified a number of developmental genes that are affected by the mutation of *HDA108* in maize. In a future study, I would like to identify genes regulated by *DSL1* and its close paralog by analyzing the transcriptome of multiple *hdac* mutants including *dsl1*, and subsequently to elucidate the developmental role of those genes in rice.

My morphological analysis indicated that several phenotypes in *dsl1* seem to be associated with cell division and proliferation. In maize, an HDAC physically interacts with a retinoblastoma-related protein that is involved in cell cycle regulation (Rossi et al. 2003). In Arabidopsis, HDA9 forms protein complex with PWR and OLI1/HOS15 that regulates cell proliferation in leaf development (Chen et al. 2016;

Kim et al. 2016; Suzuki et al. 2018). In future studies, it will be interesting to determine how *DSL1* regulates such varied developmental processes in rice, and to identify the other proteins involved in this regulation.

Chapter IV

Materials and Methods

Plant materials and growth conditions

The *dsl1* mutant (CM1322) was isolated from M_2 strains of Kinmaze mutagenized by *N*-methyl-*N*-nitrosourea. This mutant line is stocked in Kyushu University as part of the National BioResource Project. Plants were grown an NK system BioTRON (Nippon Medical and Chemical Instruments) at 28℃ or in the field.

Morphological observation and in situ hybridization

To observe rice external morphology, I used an SZX10 stereomicroscope and a DP21 camera (Olympus). For detailed phenotypic analysis, leaf blades were fixed in 4% (w/v) paraformaldehyde and 0.25% (v/v) glutaraldehyde in 0.5 M sodium phosphate buffer (pH 7.2). For observation by scanning electron microscopy (SEM), the fixed leaf blades were dehydrated in a graded ethanol series and finally replaced with 3-methylbutyl acetate. The samples were then dried at the critical point, coated with platinum, and observed under SEM (model JSM-820S; JEOL) at an accelerating voltage of 10 kV. To prepare paraffin sections, the fixed leaf blades were dehydrated in a graded ethanol/xylene series and embedded in paraffin (Paraplast Plus;

McCormick). Next, the tissues were sectioned at 8 μm with a microtome (HM355E; Microm), stained by toluidine blue, and observed under a light microscope (BX50; Olympus).

To measure the distance between small veins, I cleared leaf blades by using the transparency agent TOMEI-I (Hasegawa et al. 2016) and took photographs under a light microscope (BX50; Olympus). The distance on the photographs was then measured by using ImageJ. For observation of the SAM, shoot apices were sampled from 29-day-old plants and cleared as previously described (Suzuki et al. 2019). To check pollen viability, pollens were stained by an I_2-KI staining agent, in which 1 g of potassium iodide and 0.5 g of iodine were dissolved in 50 mL of sterile water. The stained samples were mounted in water and observed under a light microscope (BX50; Olympus).

Probes for the *CDKB2* transcript were prepared as previously described (Yasui et al. 2018). The shoot apices from 2-week-old plants embedded in paraffin were sectioned at 10 μm by using a microtome (HM355E; Microm). In situ hybridization and immunological detection were conducted as previously described (Toriba and Hirano 2018).

Isolation of the *DSL1* gene

The *dsl1* mutant was crossed with Kasalath and F_2 seeds were obtained. F_2 plants with narrow leaves were used for rough mapping. For next-generation sequencing, the genomic DNA of *dsl1* was extracted from mature leaves by using a DNeasy Plant Mini Kit (QIAGEN). DNA sequencing using MiSeq (Illumina) was performed by Hokkaido System Science (http://www.hssnet.co.jp).

To disrupt *DSL1*, a 20-bp sequence within the HDAC domain was selected as the target for guide RNA (gRNA) (Supplementary Figure S3). Synthetic oligonucleotides (5'-GTTGTGTGTCATACAAAGTCGATG-3'and 5'-AAACCATCGACTTTGTATGACACA-3') containing the target sequence were subcloned into the BbsI restriction site of the gRNA cloning vector pU6gRNA-oligo (Mikami et al. 2015). After excision from pU6gRNA-oligo, the DNA fragment including the OsU6 promoter and the gRNA region was cloned into the AscI and PacI sites of pZH_OsU3gYSA_MMCas9 (Mikami et al. 2015). This construct was introduced into T65 calli via *Agrobacterium tumefaciens* EHA101 (Hiei et al. 1994). After regeneration of plants, the target region was sequenced by using the primers 5'-ATTCTTTAGCGCCAGCCATT-3'and 5'-TGAGTAGCAAGATATGTGACAACC-3', and knockout lines of *DSL1* were identified.

Phylogenetic analysis

The sequences of the HDAC domains used for phylogenetic analysis were determined by searching in the conserved domain database (https://www.ncbi.nlm.nih.gov/Structure/cdd/wrpsb.cgi). The phylogenetic tree of the RPD3/HDA1 family was generated by using the program MEGA7 (Kumar et al. 2016). Multiple sequence alignment was performed by the MUSCLE module within MEGA7 using default parameters. The tree was constructed by the Maximum Likelihood (ML) method based on the Le_Gascuel_2008 model (LG model, (Le and Gascuel 2008)) within MEGA7. A discrete Gamma distribution was used to model differences in evolutionary rate among sites (5 categories [+G, parameter = 1.1247]). The other conditions were as follows: test of phylogeny, bootstrap method [1000 times]; gaps/missing data treatment, complete deletion; ML heuristic method, nearest-neighbor-interchange [NNI]; initial tree for ML, make initial tree automatically; branch swap filter, very strong.

RT-PCR analysis

Total RNA was isolated from Kinmaze by using TRIsure (BIOINE). First-strand cDNA was synthesized from 1 μg of total RNA using a PrimeScript™ RT Reagent

Kit (Perfect Real Time) (TaKaRa). An aliquot (3 μL) of each reverse transcription product was used for PCR using the primers 5'-GATGTGGGCAATGTCTACTTTG-3' and 5'-TCCAGAATTCCCAAAACCAG-3' for *DSL1* mRNA, and 5'-TCTGCGATAATGGAACTGGT-3' and 5'-CATAGTCCAGGGCGATGTAGG-3' for *OsACT1* mRNA.

Microarray Experiments

Shoot apices including the SAM and P1-P4 primordia were sampled from the plants at the stage when the tips of the fifth leaves were just emerged. These samples were used for RNA extraction. Total RNA was isolated with TRIsure (BIOLINE). Microarray analysis was performed using the Rice (US) gene 1.0 ST array (Thermo Fisher Scientific) as described by Yasui et al. (2018) with three biological replicates per assay. The resulting data were analyzed by rank product method (Breitling et al. 2004). GO enrichment analysis was carried out with agriGO v2.0 (Tian et al., 2017; http:// systemsbiology.cau.edu.cn/agriGOv2/).

Chapter V

Concluding remarks

My purpose in this thesis is to isolate a new gene that regulates rice development and to obtain some insights to understand the molecular mechanism of rice morphogenesis. In this study, I focused on a novel mutant, *dsl1*. I showed that the *dsl1* mutant exhibited various defects, including semi-dwarfism, small leaves, narrower intervals between the veins, an abnormal elongation pattern of internodes, and small panicles. I also revealed that *DSL1* encodes an HDAC gene in the RPD3/HDA1 family, the function of which in rice development is poorly understood. Judging from the reduction of cell number and the low expression of *CDKB2* in *dsl1*, *DSL1* seems to be involved in rice development by regulating cell cycle and cell proliferation.

Histone deacetylation is related to regulate gene expression by changing chromatin accessibility. For further analysis, it is indispensable for elucidating the target genes that are regulated by *DSL1*. To this end, I compared the transcriptome profiles in vegetative tissues between wild type and *dsl1* using microarray analysis. Then, I extracted several up-regulated and down-regulated genes in *dsl1*. Unfortunately, however, I was not able to detect any genes related to developmental

regulation.

I have two ideas to overcome this problem. The first idea is to use the multiple knockout mutants of HDACs generated by CRISPR-Cas9 technology for the transcriptome analysis. My phylogenetic analysis revealed that *DSL1* has several close homologs in rice. Therefore, the functional redundancy between *DSL1* and the homologous genes should be considered. Indeed, the phenotypes of the *dsl1* mutant seemed to be not severe in most cases. It is possible that more up-regulated and down-regulated genes can be extracted by the comparison between the multiple knockout mutants including *dsl1* and wild type. The other idea is to use the shoot apex consisting of the SAM and the younger leaf primordia (P1-P3) for transcriptome analysis. In this thesis, I used the shoot apex and the P4 leaf. Because P4 leaf occupied a large portion of a whole sample, it might obstruct the detection of the differences in the gene expression between *dsl1* and wild type. By these improvements, it is possible to find both up-regulated and down-regulated genes by *DSL1* and close HDAC genes and to elucidate the function of critical genes responsible for rice development.

After identification of both up- and down-regulated genes, it will be necessary to analyze the functions of the individual target genes of HDACs. First, it is needed

to confirm whether the down-regulated genes are related to deacetylation. For this purpose, I will perform ChIP-seq and compare the acetylation levels of those genes in wild type with that in *dsl1*. Next, to reveal the functions of the target genes, for example, I will observe the knockout mutant of the genes and examine the spatial and temporal expression of the genes. These analyses will be useful to elucidate the roles of the HDACs in rice development and to identify key genes related to unique morphology of rice.

References

Aichinger, E., Kornet, N., Friedrich, T. and Laux, T. (2012) Plant stem cell niches. *Ann. Rev. Plant Biol.* 63: 615-636.

Alinsug, M.V., Yu, C.W. and Wu, K. (2009) Phylogenetic analysis, subcellular localization, and expression patterns of RPD3/HDA1 family histone deacetylases in plants. *BMC Plant Biol.* 9: 37.

Breitling, R., Armengaud, P., Amtmann, A. and Herzyk, P. (2004) Rank products: a simple, yet powerful, new method to detect differentially regulated genes in replicated microarray experiments. *FEBS Lett.* 573: 83-92.

Chen, X., Lu, L., Mayer, K.S., Scalf, M., Qian, S. and Lomax, A. (2016) POWERDRESS interacts with HISTONE DEACETYLASE 9 to promote aging in *Arabidopsis*. *Elife* 5: e17214.

Cho, S.H., Yoo, S.C., Zhang, H., Pandeya, D., Koh, H.J., Hwang, J.Y., et al. (2013) The rice *narrow leaf2* and *narrow leaf3* loci encode WUSCHEL-related homeobox 3A (OsWOX3A) and function in leaf, spikelet, tiller and lateral root development. *New Phytol.* 198: 1071-1084.

Chung, P.J., Kim, Y.S., Jeong, J.S., Park, S.H., Nahm, B.H. and Kim, J.K. (2009) The histone deacetylase OsHDAC1 epigenetically regulates the *OsNAC6* gene that controls seedling root growth in rice. *Plant J.* 59: 764-776.

Forestan, C., Farinati, S., Rouster, J., Lassagne, H., Lauria, M., Dal Ferro, N., et al. (2018) Control of maize vegetative and reproductive development, fertility, and rRNAs silencing by *HISTONE DEACETYLASE 108*. *Genetics* 208: 1443-1466.

Fu, W., Wu, K. and Duan, J. (2007) Sequence and expression analysis of histone deacetylases in rice. *Biochem. Biophys. Res. Commun.* 356: 843-850.

Fujino, K., Matsuda, Y., Ozawa, K., Nishimura, T., Koshiba, T., Fraaije, M.W., et al. (2008) *NARROW LEAF 7* controls leaf shape mediated by auxin in rice. *Mol. Genet. Genomics* 279: 499-507.

Ha, C.M., Jun, J.H. and Fletcher, J.C. (2010) Shoot apical meristem form and function. *Curr. Top. Dev. Biol.* 91: 103-140.

Hasegawa, J., Sakamoto, Y., Nakagami, S., Aida, M., Sawa, S. and Matsunaga, S. (2016) Three-dimensional imaging of plant organs using a simple and rapid transparency technique. *Plant Cell Physiol.* 57: 462-472.

Hiei, Y., Ohta, S., Komari, T. and Kumashiro, T. (1994) Efficient transformation of rice (Oryza sativa L.) mediated by *Agrobacterium* and sequence analysis of the boundaries of the T-DNA. *Plant J.* 6: 271-282.

Hollender, C. and Liu, Z. (2008) Histone deacetylase genes in *Arabidopsis* development. *J Integr. Plant Biol.* 50: 875-885.

Honda, E., Yew, C.L., Yoshikawa, T., Sato, Y., Hibara, K.I. and Itoh, J.I. (2018) *LEAF LATERAL SYMMETRY1*, a member of the *WUSCHEL-RELATED HOMEOBOX3* gene family, regulates lateral organ development differentially from other paralogs, *NARROW LEAF2* and *NARROW LEAF3* in rice. *Plant Cell Physiol.* 59: 376-391.

Hoshikawa, K. (1989) Growing the Rice Plant: An Anatomical Monograph. Nobunkyo, Tokyo.

Hu, Y., Qin, F., Huang, L., Sun, Q., Li, C., Zhao, Y., et al. (2009) Rice histone deacetylase genes display specific expression patterns and developmental functions. *Biochem. Biophys. Res. Commun.* 388: 266-271.

Ishiwata, A., Ozawa, M., Nagasaki, H., Kato, M., Noda, Y., Yamaguchi, T., et al. (2013) Two *WUSCHEL-related homeobox* genes, *narrow leaf2* and *narrow leaf3*, control leaf width in rice. *Plant Cell Physiol.* 54: 779-792.

Itoh, J.-I., Nonomura, K.-I., Ikeda, K., Yamaki, S., Inukai, Y., Yamagishi, H., et al. (2005) Rice plant development: from zygote to spikelet. *Plant Cell Physiol.* 46: 23-47.

Jang, I.C., Pahk, Y.M., Song, S.I., Kwon, H.J., Nahm, B.H. and Kim, J.K. (2003) Structure and expression of the rice class-I type histone deacetylase genes *OsHDAC1-3*: *OsHDAC1* overexpression in transgenic plants leads to increased growth rate and altered architecture. *Plant J.* 33: 531-541.

Kadosh, D. and Struhl, K. (1998) Targeted Recruitment of the Sin3-Rpd3 Histone Deacetylase Complex Generates a Highly Localized Domain of Repressed Chromatin In Vivo. *Mol. Cell Biol.* 18: 5121-5127.

Kim, Y.J., Wang, R., Gao, L., Li, D., Xu, C., Mang, H., et al. (2016) POWERDRESS and HDA9 interact and promote histone H3 deacetylation at specific genomic sites in *Arabidopsis*. *Proc. Natl. Acad. Sci. USA* 113: 14858-14863.

Kubo, F.C., Yasui, Y., Kumamaru, T., Sato, Y. and Hirano, H.Y. (2017) Genetic analysis of rice mutants responsible for narrow leaf phenotype and reduced vein number. *Genes Genet. Syst.* 91: 235-240.

Kumar, S., Stecher, G. and Tamura, K. (2016) MEGA7: Molecular Evolutionary Genetics Analysis Version 7.0 for Bigger Datasets. *Mol Biol Evol* 33: 1870-1874.

Le, S.Q. and Gascuel, O. (2008) An improved general amino acid replacement matrix. *Mol Biol Evol* 25: 1307-1320.

Li, D.X., Chen, W.Q., Xu, Z.H. and Bai, S.N. (2015) *HISTONE DEACETYLASE6*-defective mutants show increased expression and acetylation of *ENHANCER OF TRIPTYCHON AND CAPRICE1* and *GLABRA2* with small but significant effects on root epidermis cellular pattern. *Plant Physiol.* 168: 1448-1458.

Li, M., Xiong, G., Li, R., Cui, J., Tang, D., Zhang, B., et al. (2009) Rice cellulose synthase-like D4 is essential for normal cell-wall biosynthesis and plant growth. *Plant J.* 60: 1055-1069.

Liu, C., Li, L.C., Chen, W.Q., Chen, X., Xu, Z.H. and Bai, S.N. (2013) HDA18 affects cell fate in Arabidopsis root epidermis via histone acetylation at four kinase genes. *Plant Cell* 25: 257-269.

Liu, X., Yang, S., Yu, C.W., Chen, C.Y. and Wu, K. (2016) Histone acetylation and plant development. In *Developmental signaling in plants*. Edited by Lin, C. and Luan, S. pp. 173-199. Elsevier Inc.

Liu, X., Yang, S., Zhao, M., Luo, M., Yu, C.W., Chen, C.Y., et al. (2014) Transcriptional repression by histone deacetylases in plants. *Mol. Plant* 7: 764-772.

Liu, Z. and Karmarkar, V. (2008) Groucho/Tup1 family co-repressors in plant development. *Trends Plant Sci.* 13: 137-144.

Long, J.A., Ohno, C., Smith, Z.R. and Meyerowitz, E.M. (2006) TOPLESS regulates apical embryonic fate in *Arabidopsis*. *Science* 312: 1520-1523.

Luo, M., Yu, C.W., Chen, F.F., Zhao, L., Tian, G., Liu, X., et al. (2012) Histone deacetylase HDA6 is functionally associated with AS1 in repression of *KNOX* genes in *Arabidopsis*. *PLoS Genet.* 8: e1003114.

Mikami, M., Toki, S. and Endo, M. (2015) Comparison of CRISPR/Cas9 expression constructs for efficient targeted mutagenesis in rice. *Plant Mol. Biol.* 88: 561-572.

Oikawa, T. and Kyozuka, J. (2009) Two-Step Regulation of LAX PANICLE1 Protein Accumulation in Axillary Meristem Formation in Rice. *Plant Cell* 21: 1095-1108.

Pandey, R., Muller, A., Napoli, C.A., Selinger, D.A., Pikaard, C.S., Richards, E.J., et al. (2002) Analysis of histone acetyltransferase and histone deacetylase families of *Arabidopsis thaliana* suggests functional diversification of chromatin modification among multicellular eukaryotes. *Nucleic Acids Res.* 30: 5036-5055.

Rossi, V., Locatelli, S., Lanzanova, C., Boniotti, M.B., Varotto, S., Pipal, A., et al. (2003) A maize histone deacetylase and retinoblastoma-related protein physically interact and cooperate in repressing gene transcription. *Plant Mol. Biol.* 51: 401-413.

Rossi, V., Locatelli, S., Varotto, S., Donn, G., Pirona, R., Henderson, D.A., et al. (2007) Maize histone deacetylase hda101 is involved in plant development, gene transcription, and sequence-specific modulation of histone modification of genes and repeats. *Plant Cell* 19: 1145-1162.

Rundlett, S.E., Carmen, A.A., Suka, N., Turner, B.M. and Grunstein, M. (1998) Transcriptional repression by UME6 involves deacetylation of lysine 5 of histone H4 by RPD3. *Nature* 392: 831-835.

Sasaki, A., Ashikari, M., Ueguchi-Tanaka, M., Itoh, H., Nishimura, A., Swapan, D., et al. (2002) Green revolution: a mutant gibberellin-synthesis gene in rice. *Nature* 416: 701-702.

Sato, Y., Sentoku, N., Miura, Y., Hirochika, H., Kitano, H. and Matsuoka, M. (1999) Loss-of-function mutations in the rice homeobox gene *OSH15* affect the architecture of internodes resulting in dwarf plants. *EMBO J.* 18: 992-1002.

Somssich, M., Je, B.I., Simon, R. and Jackson, D. (2016) CLAVATA-WUSCHEL signaling in the shoot meristem. *Development* 143: 3238-3248.

Song, X.J., Kuroha, T., Ayano, M., Furuta, T., Nagai, K., Komeda, N., et al. (2015) Rare allele of a previously unidentified histone H4 acetyltransferase enhances grain weight, yield, and plant biomass in rice. *Proc. Natl. Acad. Sci. USA* 112: 76-81.

Suzuki, C., Tanaka, W. and Hirano, H.Y. (2019) Transcriptional Corepressor ASP1 and CLV-Like Signaling Regulate Meristem Maintenance in Rice. *Plant Physiol.* 180: 1520-1534.

Suzuki, M., Shinozuka, N., Hirakata, T., Nakata, M.T., Demura, T., Tsukaya, H., et al. (2018) *OLIGOCELLULA1/HIGH EXPRESSION OF OSMOTICALLY RESPONSIVE GENES15* promotes cell proliferation with *HISTONE DEACETYLASE9* and *POWERDRESS* during leaf development in *Arabidopsis thaliana*. *Frontiers Plant Sci.* 9: 1188.

Tanaka, M., Kikuchi, A. and Kamada, H. (2008) The Arabidopsis histone deacetylases HDA6 and HDA19 contribute to the repression of embryonic properties after germination. *Plant Physiol.* 146: 149-161.

Tanaka, W., Pautler, M., Jackson, D. and Hirano, H.Y. (2013) Grass meristems II: inflorescence architecture, flower development and meristem gate. *Plant Cell Physiol.* 54: 313-324.

Tian, T., Liu, Y., Yan, H., You, Q., Yi, X., Du, Z., et al. (2017) agriGO v2.0: a GO analysis toolkit for the agricultural community, 2017 update. *Nucleic Acids Res.* 45: W122-W129.

Toriba, T. and Hirano, H.-Y. (2018) Two-color in situ hybridization: a technique for simultaneous detection of transcripts from different loci. In *Plant Transcription Factors: Methods and Protocols*. Edited by Yamaguchi, N. pp. 269-287. Springer New York, New York, NY.

Woo, Y.M., Park, H.J., Su'udi, M., Yang, J.I., Park, J.J., Back, K., et al. (2007) Constitutively wilted 1, a member of the rice YUCCA gene family, is required for maintaining water homeostasis and an appropriate root to shoot ratio. *Plant Mol. Biol.* 65: 125-136.

Yamamuro, C., Ihara, Y., Wu, X., Noguchi, T., Fujioka, S., Takatsuto, S., et al. (2000) Loss of function of a rice *brassinosteroid insensitive1* homolog prevents internode elongation and bending of the lamina joint. *Plant Cell* 12: 1591-1606.

Yasui, Y., Ohmori, Y., Takebayashi, Y., Sakakibara, H. and Hirano, H.Y. (2018) *WUSCHEL-RELATED HOMEOBOX4* acts as a key regulator in early leaf development in rice. *PLoS Genet.* 14: e1007365.

Yoshida, A., Ohmori, Y., Kitano, H., Taguchi-Shiobara, F. and Hirano, H.-Y. (2012) *ABERRANT SPIKELET AND PANICLE1*, encoding a TOPLESS-related transcriptional co-repressor, is involved in the regulation of meristem fate in rice. *Plant J.* 70: 327-339.

Yoshida, A., Sasao, M., Yasuno, N., Takagi, K., Daimon, Y., Chen, R., et al. (2013) *TAWAWA1*, a regulator of rice inflorescence architecture, functions through the suppression of meristem phase transition. *Proc. Natl. Acad. Sci. USA* 110: 767-772.

Yoshikawa, T., Eiguchi, M., Hibara, K., Ito, J. and Nagato, Y. (2013) Rice *SLENDER LEAF 1* gene encodes cellulose synthase-like D4 and is specifically expressed in M-phase cells to regulate cell proliferation. *J Exp. Bot.* 64: 2049-2061.